Molecular Neurobiology (2019) 56:6521–6538
https://doi.org/10.1007/s12035-019-1539-9

Canonical Wnt Pathway Maintains Blood-Brain Barrier Integrity upon Ischemic Stroke and Its Activation Ameliorates Tissue Plasminogen Activator Therapy

Noëmie Jean LeBlanc[1,2] · Romain Menet[1,2] · Katherine Picard[1,3] · Geneviève Parent[1,3] · Marie-Ève Tremblay[1,3] · Ayman ElAli[1,2]

Received: 20 November 2018 / Accepted: 22 February 2019 / Published online: 9 March 2019

Abstract

Stroke induces blood-brain barrier (BBB) breakdown, which promotes complications like oedema and hemorrhagic transformation. Administration of recombinant tissue plasminogen activator (rtPA) within a therapeutic time window of 4.5 h after stroke onset constitutes the only existing treatment. Beyond this time window, rtPA worsens BBB breakdown. Canonical Wnt pathway induces BBB formation and maturation during ontogeny. We hypothesized that the pathway is required to maintain BBB functions after stroke; thus, its activation might improve rtPA therapy. Therefore, we first assessed pathway activity in the brain of mice subjected to transient middle cerebral artery occlusion (MCAo). Next, we evaluated the effect of pathway deactivation early after stroke onset on BBB functions. Finally, we assessed the impact of pathway activation on BBB breakdown associated to delayed administration of rtPA. Our results show that pathway activity is induced predominately in endothelial cells early after ischemic stroke. Early deactivation of the pathway using a potent inhibitor, XAV939, aggravates BBB breakdown and increases hemorrhagic transformation incidence. On the other hand, pathway activation using a potent activator, 6-bromoindirubin-3′-oxime (6-BIO), reduces the incidence of hemorrhagic transformation associated to delayed rtPA administration by attenuating BBB breakdown via promotion of tight junction formation and repressing endothelial basal permeability independently of rtPA proteolytic activity. BBB preservation upon pathway activation limited the deleterious effects of delayed rtPA administration. Our study demonstrates that activation of the canonical Wnt pathway constitutes a clinically relevant strategy to extend the therapeutic time window of rtPA by attenuating BBB breakdown via regulation of BBB-specific mechanisms.

Keywords Ischemic stroke · Hemorrhagic transformation · Blood-brain barrier · Brain endothelial cells · Tissue plasminogen activator · Canonical Wnt pathway · Tight junctions

Introduction

Stroke constitutes a major cause of death and disability of the adult population in the industrialized world. Ischemic stroke, which occurs as a result of a sudden obstruction within a cerebral artery due to an embolus or thrombus, accounts for the majority of cases [1]. The remaining cases are hemorrhagic and occur when a cerebral artery suddenly ruptures [2]. Brain endothelial cells, which form the blood-brain barrier (BBB), are tightly sealed together via tight junctions that limit the unspecific entry of blood-borne molecules and immune cells into the brain, and express several sophisticated transport systems that orchestrate the uptake of nutrients and the elimination of toxic metabolites [3]. Ischemic stroke triggers BBB breakdown via destabilization of the tight junctions and deregulation of the transport mechanisms in its acute phase [4, 5]. BBB breakdown contributes to the progression of secondary brain injury by causing oedema formation, increasing the accumulation of toxic metabolites, and exacerbating the inflammatory response [6]. Severity of these events exacerbates acute ischemic stroke injury, and worsens post-stroke deficits

✉ Ayman ElAli
ayman.el-ali@crchudequebec.ulaval.ca

[1] Neuroscience Axis, Research Center of CHU de Québec - Université Laval, 2705 Laurier Boulevard, Quebec City, QC G1V 4G2, Canada

[2] Department of Psychiatry and Neuroscience, Faculty of Medicine, Université Laval, Québec City, QC, Canada

[3] Department of Molecular Medicine, Faculty of Medicine, Université Laval, Québec City, QC, Canada

by reducing the capacity of brain to regenerate and recover [1, 7, 8].

Currently, recombinant tissue plasminogen activator (rtPA)–induced thrombolysis is the only Food and Drug Administration (FDA)–approved approach used in clinics to restore cerebral blood flow (CBF) [9]. Nonetheless, rtPA should be administered within a very narrow time window of 4.5 h after stroke onset [10]. Consequently, less than 5% of eligible stroke patients can benefit from thrombolysis [9]. Beyond this time window, rtPA causes neurotoxicity and hemorrhagic transformation, which jointly aggravate tissue injury [9]. Hemorrhagic transformation constitutes a major complication of ischemic stroke, causing significant morbidity and mortality in patients [11, 12]. Hemorrhagic transformation occurs, at least partly, as a result of BBB breakdown aggravation, essentially due to activation of the matrix metalloproteinases (MMPs) [9]. As rtPA is an already an FDA-approved drug, developing strategies to extend its therapeutic window and reduce the risk associated to its administration through BBB preservation constitutes a highly promising bench-to-clinic therapeutic avenue.

The evolutionarily conserved canonical Wnt pathway (i.e., called Wnt/β-catenin pathway), which regulates crucial aspects of cell biology during development [13], was recently demonstrated to orchestrate BBB formation and maturation during ontogeny [14]. Wnt proteins, which are secreted by astrocytes and neurons, activate an endothelial receptor complex formed by Frizzled (Fzd) and LRP5/6 receptors, stabilizing β-catenin in the cytosol [3]. Subsequently, β-catenin translocates to the nucleus and binds the lymphoid enhancer factor (LEF)/T cell factor (TCF) transcription factor to specifically induce expression of the tight junction protein claudin-3, and represses expression of the plasmalemma vesicle associated protein (PLVAP) that is involved in brain endothelial cell permeability [3, 14]. Although minimally active in the adult brain vasculature, the pathway remains essential for maintaining BBB integrity throughout the lifespan [15]. However, pathway activity seems to be deregulated in several brain disorders [16]. Little is known about how the pathway is regulated in brain endothelial cells upon ischemic stroke. Nonetheless, the canonical Wnt pathway was reported to be specifically deactivated in endothelial cells located near the bleeding sites in the brain of hemorrhagic stroke patients, translated by low levels of β-catenin in endothelial cells [15], outlining a potential role of the pathway in preventing hemorrhages under pathological conditions.

In view of its role as a master regulator of BBB structural and functional integrity at the transcriptional level [3], we were interested in investigating how canonical Wnt pathway affects BBB integrity and consequently rtPA therapy upon acute ischemic stroke. In this study, we have first analyzed pathway activity in the acute phase of ischemic stroke in mice subjected to transient middle cerebral artery occlusion (MCAo), and evaluated the impact of pathway activity modulation on BBB integrity and delayed administration of rtPA. Our data show that early pathway deactivation using the potent inhibitor XAV939 aggravates BBB breakdown and increases the incidence of spontaneous hemorrhagic transformation. On the other hand, pathway activation using a potent agonist, 6-bromoindirubin-3′-oxime (6-BIO), attenuates BBB breakdown and reduces the incidence of hemorrhagic transformation associated to delayed rtPA administration. Pathway activation restores the expression of claudin-3/5, and attenuates basal endothelial permeability by repressing PLVAP expression, without affecting vascularization and inflammation. These effects were accompanied by a reduced degeneration of neurons in the hippocampus. Our study demonstrates that activation of the canonical Wnt pathway constitutes a clinically relevant strategy to extend the therapeutic window of rtPA by attenuating BBB breakdown via regulation of BBB-specific mechanisms.

Materials and Methods

Animal Experiments

Animal experiments were performed according to the Canadian Council on Animal Care guidelines, as administered by the Université Laval Animal Welfare Committee. Mice were housed and acclimated to standard laboratory conditions (12-h light/dark cycle, lights on at 7:00 AM and off at 7:00 PM) with free access to chow and water. Adult C57BL6/j male mice (3 months old) were subjected to focal ischemic stroke via the transient occlusion of the MCA using an intraluminal filament technique as described [17]. Briefly, mice were anesthetized under 1.5% isoflurane (30% O_2, remainder N_2O) and body temperature was maintained between 36 and 37 °C using a feedback-controlled heating system (Harvard Apparatus, QC, Canada) throughout surgery. After a midline neck incision, the left common and external carotid arteries were isolated under a microscope and ligated. A microvascular clip was placed on the internal carotid artery and a 7–0 silicon-coated nylon monofilament (Doccol Corporation, MA, USA) was directed through the internal carotid artery until the origin of MCA. The monofilament was left in place for 30 min and then withdrawn. During the experiment, laser Doppler flow (LDF) was monitored using a flexible fiber-optic probe (Moor Instruments Inc., DE, USA) attached to the skull overlying the core of the MCA territory. For the experiments assessing pathway pharmacological deactivation of the canonical Wnt pathway, a first group of mice received injections of (a) vehicle (10% dimethyl sulfoxide (DMSO); intraperitoneal), and (b) XAV939 (40 mg/kg; intraperitoneal) (Sigma-Aldrich, St. Louis, MO, USA) one dose immediately after MCAo. XAV939 dosage to efficaciously deactivate the

pathway in the mouse brain was chosen based dose-response studies and published reports [18]. For experiments evaluating the effects of delayed rtPA administration and pathway pharmacological activation, a second set of mice received intravenous bolus injections of (a) saline (0.9% NaCl), and (b) rtPA (alteplase) (10 mg/kg; Genentech, CA, USA) one dose 6 h after MCAo induction. Animals were randomly assigned to 4 groups, each of which was treated with (a) vehicle (10% DMSO; intraperitoneal), (b) 6-BIO (1 mg/kg; intraperitoneal) (Selleck Chemicals, TX, USA) 2 doses 3 and 6 h after MCAo induction. 6-BIO dosage to efficaciously activate the pathway in the mouse brain was chosen based dose-response studies and published reports [19]. For transmission electron microscopy (TEM) experiments, a sub-group of animals were injected intravenously 30 min before perfusion with horseradish peroxidase (HRP) (0.5 g/kg; Sigma-Aldrich).

Assessment of Neurological Deficits

Neurological deficits were monitored 24 h after MCAo induction, as previously described [20]. The sensorimotor performance of mice subjected to MCAo was assessed using a widely used neurological score test that closely correlates the deficits with the overall severity of the histological injury. Neurological deficits were evaluated using the following score: 0 = normal function; 1 = mild circling behavior with attempts to rotate to the contralateral side upon lifting of the animal by the tail; 2 = circling to the contralateral side but normal posture at rest; 3 = reclination and consistent circling to the contralateral side at rest, with mouse nose almost reaching its tail; and 4 = absence of spontaneous motor activity.

Tissue Processing

Twenty-four hours after surgery, mice were sacrificed via a transcardiac perfusion. For immunohistochemical and histochemical studies, a sub-group of mice was euthanized via a cardiac perfusion with ice-cold 0.9% NaCl solution followed by 4% paraformaldehyde (PFA), as previously described [20]. Brains were removed and cut on microtome into 25-μm coronal sections that were kept in an anti-freeze solution (30% glycerol, 30% ethylene glycol in 0.9% NaCl, phosphate buffer (PB)) at − 20 °C for further use. For molecular studies, another sub-group of mice was euthanized via transcardiac perfusion with ice-cold 0.9% NaCl. Brains were removed and were snap-frozen on dry ice and kept at − 80 °C until further use.

Transmission Electron Microscopy

TEM imaging of a sub-group of saline-, rtPA-, and rtPA/6-BIO-treated mice was performed as previously described [21, 22]. Briefly, 10 mg (per 20 g of body weight) of HRP (Sigma-Aldrich) was dissolved in 0.4 ml of PBS and injected into the tail veins of mice. After 30 min of HRP circulation, mice were deeply anesthetized with sodium pentobarbital (80 mg/kg; intraperitoneal). They were then perfused through the aortic arch with 3.5% acrolein (in 100 mM phosphate buffer, pH 7.4) followed by 4% PFA (in 100 mM PB, pH 7.4). Brains were removed, cut into 50-μm transverse sections with a vibratome (Leica VT1000S) in ice-cold phosphate-buffered saline (PBS; 0.9% NaCl in 50 mM phosphate buffer, pH 7.4), and kept in anti-freeze solution at − 20 °C. Sections were washed in PBS and developed using diaminobenzidine (DAB) solution (0.05% DAB, 0.015% H_2O_2 in Tris-buffered solution [TB; 50 mM at pH 8.0]) for 45 min at room temperature. Sections were then fixed in a mixture of 3% potassium ferrocyanide and 2% osmium tetroxide in PB for 1 h. Afterwards, sections were incubated in thiohydracarbazine (TCH; 10 mg/ml in H_2O) for 20 min. After washing, they were fixed again in 2% osmium tetroxide in H_2O for 30 min. After the second osmium incubation, sections were dehydrated in ascending concentrations of ethanol followed by three washes of 5 min in propylene oxide. For resin embedding, brain sections were immersed in Durcupan (Electron Microscopy Science (EMS), PA, USA) for 24 h at room temperature. The following day, they were placed between two ACLAR sheets (EMS) and kept at 55 °C for 72 h. For each animal, a trapezoid was cut off from the striatum of the ACLAR sheet, and then glued on top of a resin block. Ultrathin sections of approximately 75 nm thick were sliced with an ultramicrotome (Leica Ultracut S), collected on copper 200-mesh grids (EMS), and examined with a Tecnai G2 Spirit Biotwin transmission electron microscope. For each animal, pictures of capillaries were randomly taken at a magnification of × 4800 and × 13,000 using a digital camera ORCA-HR (10 MP; Hamamatsu, Japan). HRP inclusions were counted in the brain cells constituting the neurovascular unit (endothelial cells, pericytes, and astrocytes) with Photoshop software (CC 2018, Adobe). The investigator was blinded to the experimental conditions during imaging and analysis.

Isolation of Brain Capillaries

Brain capillaries from contralateral and ipsilateral hemispheres were isolated on dextran gradient as described [4]. Briefly, contralateral and ipsilateral hemispheres of each animal were separated; the MCAo region of the ipsilateral (striatum and overlaying cortex) was dissected and a similar region on the contralateral hemisphere was dissected as well. The samples were gently homogenized in a Teflon glass homogenizer in ice-cold microvessel isolation buffer (MIB; 15 mM HEPES, 147 mM NaCl, 4 mM KCl, 3 mM $CaCl_2$, and 12 mM $MgCl_2$) supplemented with 1% protease inhibitor cocktail (Sigma-Aldrich) and 1% phosphatase inhibitor cocktail 2 (Sigma-Aldrich). Homogenates were centrifuged at

1000*g* for 10 min at 4 °C. The resulting pellets were re-suspended in 30% dextran (molecular weight 64,000 to 76,000; Sigma-Aldrich) in MIB. Suspensions were centrifuged at 3700*g* for 20 min at 4 °C. The resulting crude brain capillaries-rich pellets were re-suspended in MIB, centrifuged again, and lysated in NP40 lysis buffer supplemented with 1% protease inhibitor cocktail (Sigma-Aldrich) and 1% phosphatase inhibitor cocktail (Sigma-Aldrich). Lysated samples were sonicated over 3 cycles lasting 45 s each. Protein concentration was measured using the bicinchoninic acid (BCA) method (QuantiPro assay kit, Sigma-Aldrich). Brain capillaries were stored at − 80 °C until further use.

Analysis of Brain Injury, IgG Extravasation, and Hemorrhagic Transformation

Representative free-floating brain sections were mounted onto SuperFrost slides (Fisher Scientific, Ottawa, ON, Canada) and thorough overnight dried under vacuum. Sections were next stained with 0.5% cresyl violet to assess the brain infarct size, as previously described [23]. Stained sections were digitized and the border between injured and non-injured healthy tissue was outlined with ImageJ analysis software (National Institutes of Health, Bethesda, MD, USA). The infarct size was measured by subtracting the area of the ipsilateral hemisphere from that of the contralateral hemisphere. Adjacent sections were processed for immunohistochemistry to stain infiltration of the serum immunoglobulin G (IgG), an endogenous marker of BBB breakdown, as previously described [23]. Briefly, mounted brain sections were washed with potassium phosphate-buffered saline (KPBS) (Sigma-Aldrich) and then incubated for 20 min in a permeabilization/blocking solution containing 4% normal goat serum (NGS), 1% bovine serum albumin (BSA) (Sigma-Aldrich), and 0.4% Triton X-100 (Sigma-Aldrich) in KPBS. Biotinylated anti-mouse IgG antibody (Santa Cruz Biotechnology, Dallas, TX, USA) was incubated overnight at 4 °C. Staining was revealed using an avidin peroxidase kit (Vectastain Elite; Vector Labs, Burlingame, CA, USA) by immersing brain sections for 1 h in Avidin-Biotin Complex (ABC) mixture. Brain sections were washed and stained in DAB solution for 10 min, and washed again. Slices were mounted onto slides, dried, dehydrated, and overlaid with coverslips using distyrene plasticizer xylene (DPX) mounting solutions. Brain sections were digitized and analyzed for areas exhibiting IgG extravasation using ImageJ software. For assessment of hemorrhagic transformations, sections were directly incubated with DAB solution for 10 min and then washed in KPBS to stain the naturally trapped erythrocytes and permit visualization of ruptured microvessels presenting perivascular petechial bleeding. Sections were processed the same as for the IgG staining. The number of ruptured microvessels in each group was counted. Hemorrhagic transformation incidence was calculated as ratio of the number of ruptured microvessels in the different experimental groups divided by the mean value of the number of ruptured microvessels in control groups.

Fluoro-Jade B Staining

Fluoro-jade B (FJB) staining was used as an indicator of neuronal death as described [24]. Mounted free-floating brain sections were fixed with 4% PFA for 20 min. Fixed sections were then rinsed twice with KPBS for 5 min and processed through a cycle of dehydration/rehydration in ethanol at different dilutions as follows: 3 min in 50%, 1 min in 70%, 3 min in 100%, 1 min in 70%, 1 min in 50%, and 1 min in distilled water. Mounted sections were next treated for 10 min with 0.06% potassium permanganate (MP Biomedicals, Santa Ana, CA, USA), rinsed for 1 min with distilled water and then incubated in 0.0004% FJB solution (EMD Millipore, Etobicoke, ON, Canada) containing 0.1% acetic acid and 2 μg/ml DAPI. Sections were dried overnight, immersed in xylene, and then cover-slipped in anti-fade mounting solution (Sigma-Aldrich). Fluorescent images were taken using a Nikon C80i microscope (Nikon Instruments, Williston, VT, USA) equipped with a motorized stage (Ludl, Hawthorne, NY, USA) and QImaging® color camera (MBF 2000 R, Quantitative Imaging, Surrey, BC, Canada) using QCapture Version 2.98.2 software (Quantitative Imaging).

ELISA Assays

The protein levels of β-catenin in isolated brain capillaries from the ipsilateral hemisphere were assessed using the mouse β-catenin ELISA kit (Abcam). The experimental procedure for mouse β-catenin detection was performed according to the manufacturer's instructions. Briefly, brains were homogenized in ice-cold lysis buffer, and centrifuged at 2500*g* for 10 min at 4 °C. Supernatant was diluted and loaded into a 96-well microplate. Absorbance was acquired using a microtiter plate reader using a 450-nm wavelength filter (SpectraMax i3, Molecular Devices, San Diego, CA, USA), and analyzed using SOFTmax Pro 6.4.0.1 software (Molecular Devices). To assess the accumulation of blood-derived rtPA in the ischemic brain, the human rtPA Platinum ELISA kit (Thermo Fisher Scientific, MA, USA) was used according to the manufacturer's instructions. The kit allows detection of free and complexed human rtPA, and does not cross react with endogenous murine rtPA. Brain homogenates were loaded into the 96-well microplate. Absorbance was acquired using a microtiter plate reader using a 450-nm wavelength filter as specified before. Optical density (OD) values were corrected for the total protein quantity in each sample. Human rtPA relative quantities were represented as OD at 495 nm/mg total brain homogenates.

Western Blot Analysis

Protein samples (20 μg) were mixed with 5× sodium dodecyl sulfate (SDS)–loading buffer and heated for 5 min at 95 °C. Samples were subjected to 10%, 12%, 15%, or 17% SDS polyacrylamide gel electrophoresis (SDS-PAGE), and subjected to electrophoresis using Mini-PROTEAN® Tetra Cell (Bio-Rad, Hercules, CA, USA). After migration, resolved protein bands were transferred onto a 0.45-μm polyvinylidene fluoride (PVDF) membrane (EMD Millipore) for 1 h on ice using Mini Trans-Blot® Electrophoretic Transfer Cell (Bio-Rad). The PVDF membrane was rinsed three times with a 0.1 M Tris-buffered saline solution containing 0.5% Tween-20 (TBS-T; Sigma-Aldrich) and blocked in TBS-Tween with 5% (*w*/*v*) skim milk for 30 min at room temperature. The PVDF membrane was then incubated overnight at 4 °C with different primary antibodies diluted at 1/1000 in TBS-T solution. The following antibodies were used: rabbit anti-β-catenin (9562S; Cell Signaling Technology, Danvers, MA, USA), rabbit anti-PLVAP (14452-1-AP; Proteintech group, Rosemont, IL, USA), rabbit anti-claudin-5 (ab15106; Abcam), and mouse anti-β-actin (MAB1501; EMD Millipore). Primary antibodies were detected with the appropriate horseradish peroxidase (HRP)–conjugated secondary antibodies (Jackson Immunoresearch, West Grove, PA, USA) that were diluted 1/10000 in TBS-T and revealed by enhanced chemiluminescence plus (ECL) solution (Bio-Rad, Hercules, CA, USA). β-actin was used to ensure equal protein loading. Blots were revealed and immediately digitized using Thermo Scientific myECL Imager (Thermo Fisher Scientific, Waltham, MA, USA). Digitized blots were densitometrically analyzed with ImageJ software, corrected for protein loading by means of β-actin or Lamin B1, and expressed as relative values comparing different groups.

Immunofluorescence Analysis

Mounted sections were first incubated for 20 min in a permeabilization/blocking solution containing 4% NGS, 1% BSA, and 0.4% Triton X-100 in KPBS, and then overnight at 4 °C with different primary antibodies diluted in the same solution. The following primary antibodies were used: rat anti-CD31 (550274; 1/500; BD Biosciences, San Jose, CA, USA), rabbit anti-ionized calcium binding adaptor molecule-1 (Iba1;019-19741; 1/250; Wako Chemicals, Cape Charles, VA, USA), mouse anti-active β-catenin specifically recognizing the dephosphorylated amino acids on Serine 37 or Threonine 41 (05-665; 1/250, EMD Millipore), and rabbit anti-claudin-3 (34-1700; 1/250, Invitrogen, Carlsbad, CA). Sections were then rinsed in KPBS and incubated for 2 h with one the following secondary antibodies: Alexa Fluor 488–conjugated goat anti-rat antibody (Invitrogen), Alexa Fluor 488–conjugated goat anti-mouse antibody (Invitrogen), Cy3 AffiniPure goat anti-rabbit IgG (H+L) (Jackson Immunoresearch), and Cy3 AffiniPure goat anti-mouse IgG (H+L) (Jackson Immunoresearch). After another washing step with KPBS, sections were cover-slipped with anti-fade mounting medium (Sigma-Aldrich). Epifluorescence images were taken using a Nikon C80i microscope equipped with a motorized stage (Ludl) and a QImaging® color camera (Quantitative Imaging) using QCapture Version 2.98.2 software (Quantitative Imaging). Confocal laser scanning microscopy was performed with a LSM 800 microscope equipped with the ZEN Imaging Software (Carl Zeiss Canada, Toronto, ON, Canada). To investigate expression of active β-catenin and claudin-3 in brain sections, the number of β-catenin$^+$ and claudin-3$^+$ structures was assessed respectively, using unbiased computer-assisted stereological quantification (Stereo Investigator; MBF Bioscience, VT, USA). To evaluate β-catenin density and claudin-3 disruption, the length of β-catenin vascular-like and claudin-3 structures were evaluated using computer-assisted stereological quantification.

Gelatinase Activity Assay

To investigate the enzymatic activity of MMP-2/9 (gelatinase), we used a highly sensitive fluorescent-based assay "EnzCheck® Gelatinase/Collagenase Assay Kit" (Molecular Probes, Eugene, OR, USA). The gelatinase assay was performed in the black 96-well plate according to manufacturer's protocol [25]. Briefly, 80 μl of reaction buffer and 20 μl of a solution that contains DQ™ gelatin at a concentration of 100 μg/ml were added to each well. To evaluate the gelatinase activity of MMP-2/9 activity in the ischemic brain, 30 μg of proteins extracted from total brain homogenates samples was added to each well and completed with reaction buffer to 200-μl final volume. Following incubation for 24 h at room temperature, fluorescence was measured using a microplate reader (SpectraMax i3, Molecular Devices) set for excitation at 485 ± 10 nm and emission detection at 530 ± 15 nm. Background fluorescence has been subtracted from each value. Gelatinase activity is proportional to the relative fluorescence intensity, which that was analyzed using SOFTmax Pro6.4 software (Molecular Devices) [25]. Gelatinase relative activity was represented as relative fluorescence unit (RFU).

Cell-Based Assays

Cell Culture We chose immortalized murine brain-derived endothelial cells (bEnd3) (ATCC, Manassas, VA, USA) to represent brain endothelial cells, as these cells have been shown to have similar barrier characteristics to primary brain microvascular endothelial cells (BEMC) [26]. Moreover, bEnd3 cells are attractive candidates to represent the cellular component of the BBB, and are amenable to numerous molecular

interventions [25]. bEnd3 cells were cultured at 37 °C in 5% CO_2, 95% air in DMEM glucose–normal medium (Multicell, Wisent) containing 10% FBS, 2 mM L-glutamine, 100 U/ml penicillin, and 100 μg/ml streptomycin. In all experiments, cells were grown to approximately 80% confluence, and subjected to a maximum of 8 cell passages. To further confirm some observations related to regulation of key BBB markers, we have used primary microvascular endothelial cells that were isolated from the brain of 6-week-old C57BL6/j mice (generous gift from Dr. Steve Lacroix, Université Laval). In these experiments, primary brain endothelial cells were grown to approximately 80% confluence in the collagen-IV-coated 6-well microplate. Cells at passage 2 were used for pharmacological stimulation.

Dose-Response Studies bEnd3 cells were seeded at 2×10^5 cells/well in a 12-well plate (Corning, NY, USA). Cells were treated with saline, 2.5 μM, 5 μM, or 15 μM of 6-BIO. As screening experiments showed that 6-BIO at 5 μM was more efficient, this dose was adopted to perform the functional studies. At the end of each experiment, cells were harvested for protein extraction and further analysis. Nuclear proteins were obtained from the bEnd3 cells using a Nuclear Extraction Kit (Abcam Inc., Toronto, ON, Canada) according to the manufacturer's instructions. The cytoplasmic part was obtained from the same protocol as well.

OGD Induction To investigate the responses of brain endothelial cells challenged by ischemia/reperfusion-like conditions, cells were incubated in oxygen- and glucose-deprived (OGD) conditions, as previously described [20]. OGD was induced by incubating cells at 37 °C in a Dulbecco's modified Eagle's medium (DMEM) glucose–free medium (Multicell, Wisent, St-Bruno, QC, Canada) under hypoxic condition (1% O_2) for 6 h (ischemia-like) using a Modular Incubator Chamber (Billups-Rothenberg Inc., Del Mar, CA, USA). Following the 6 h OGD, DMEM glucose–free medium was immediately replaced by DMEM glucose–normal medium and cells were incubated under normal oxygenation conditions to allow a re-oxygenation period (reperfusion-like) for 24 h as specified in different experiments. As control, cells were incubated at 37 °C in DMEM glucose–normal medium (Multicell, Wisent) under normal oxygenation conditions (normoxia). Cells were treated with 5 μM 6-BIO at 3 and 6 h following OGD or 20 μg/ml rtPA 6 h following OGD. Control groups were treated with the same volume of either DMSO or 0.9% NaCl solution. Cells were harvested 24 h after incubation for protein extraction using NP40 lysis buffer supplemented with 1% protease inhibitor cocktail (Sigma-Aldrich) and 1% phosphatase inhibitor cocktail (Sigma-Aldrich), as specified before. Lysates were sonicated over 2 cycles lasting 20 s each at 4 °C at 40% power. Protein concentrations were determined using the BCA method (QuantiPro assay kit, Sigma-Aldrich). To simplify, we used throughout the text OGD instead of OGD/re-oxygenation.

Endothelial Permeability Assay The para-cellular permeability of bEnd.3 cells was assessed via measurement of the diffusion of fluorescein sodium salt (NaF; 4 kDa; Sigma-Aldrich) across a monolayer of bEnd.3 cells as previously described [27]. Briefly, bEnd3 cells were seeded at a density of 5×10^4 cells/transwell in culture media onto the upper "apical" chamber of tissue culture inserts (Millicell Hanging Cell Culture Insert, translucent polyethylene terephthalate (PET) 0.4-μm pore size; EMD Millipore) and cultured to be 85% confluent. Culture media were replenished in the upper and lower chambers every 24 h. Two days post-confluence, bEnd3 were then placed under OGD conditions for 6 h. Afterwards, DMEM glucose–free medium was immediately replaced by DMEM glucose–normal medium and cells were incubated under normal oxygenation conditions to allow reperfusion. Immediately following reperfusion, cells were either treated with 6-BIO (5 μM) at 3 and 6 h after reperfusion, rtPA (20 μg/ml) at 6 h after reperfusion, or a mix of both. Controls were treated with the same volume of either DMSO or saline. After 24 h of incubation, the inserts were transferred into fresh wells containing pre-warmed Krebs-HEPES buffer (composed of [in mmol/l] 99 NaCl; 4.7 KCl; 1.2 $MgSO_4$; 1.0 KH_2PO_4; 19.6 $NaHCO_3$; 11.2 glucose; 20 Na-HEPES; 2.5 $CaCl_2$, pH 7.4). The inserts were washed twice with pre-warmed Krebs-HEPES buffer, and then NaF (200 μg/ml) was added to the upper chamber and left to incubate for 60 min at 37 °C. Twenty-five microliters of samples was collected from the apical and lower compartment and transferred into a black 96-well plate to measure fluorescence (492/518 nm, absorption/emission wavelengths) using SpectraMax i3 (Molecular Devices, San Diego, CA, USA) and analyzed using SOFTmax Pro 6.4.0.1 software (Molecular Devices). Fluorescent results are corrected using the fluorescence of the lower compartment to eliminate any variability due to a change in volume between wells.

Statistical Analysis

Results are expressed as mean ± standard error of the mean (SEM). For comparisons between two groups, unpaired two-tailed Student's *t* test was used. For comparisons of multiple groups, ordinary one-way analysis of variance (ANOVA) followed by Tukey's post hoc test and Kruskal-Wallis ANOVA followed by the Dunn post hoc test were used. *P* values lower than 0.05 were considered significant. All statistical analyses were performed using GraphPad Prism Version 6 for Windows (GraphPad Software, San Diego, CA, USA).

Results

Pathway Activity Is Detectible Predominately in the Brain Endothelial Cells and Re-Emerges upon Ischemic Stroke

Canonical Wnt pathway activity is very low in the adult brain, but re-emerges in response to neuroinflammatory diseases. To evaluate the activity status of the pathway in the brain upon ischemic stroke, spatiotemporal analysis of β-catenin expression was performed using an antibody that specifically recognizes the active form of β-catenin, dephosphorylated on Serine 37, or Threonine 41 [28]. Noticeably, β-catenin was predominantly expressed in brain endothelial cells ($CD31^+$ cells), and was barely expressed in other brain cells (Fig. 1a, c). Importantly, β-catenin expression was potently induced in the ischemic brain endothelial cells as early as 3 h after MCAo induction (Fig. 1a, b), and stayed elevated 24 h after but to a lesser extent (Fig. 1c, d). These results indicate that ischemic stroke triggers re-emergence of pathway activity specifically in brain endothelial cells very early, a response that decreases over time.

Early Pathway Deactivation Aggravates BBB Breakdown and Increases Incidence of Spontaneous Hemorrhagic Transformation

To understand the biological significance of canonical Wnt pathway activity re-emergence in brain endothelial cells upon ischemic stroke, the pathway was deactivated via systemic administration of XAV939 immediately after MCAo induction. XAV939 was administered systemically to allow optimal accumulation within the ischemic leaky vasculature, while

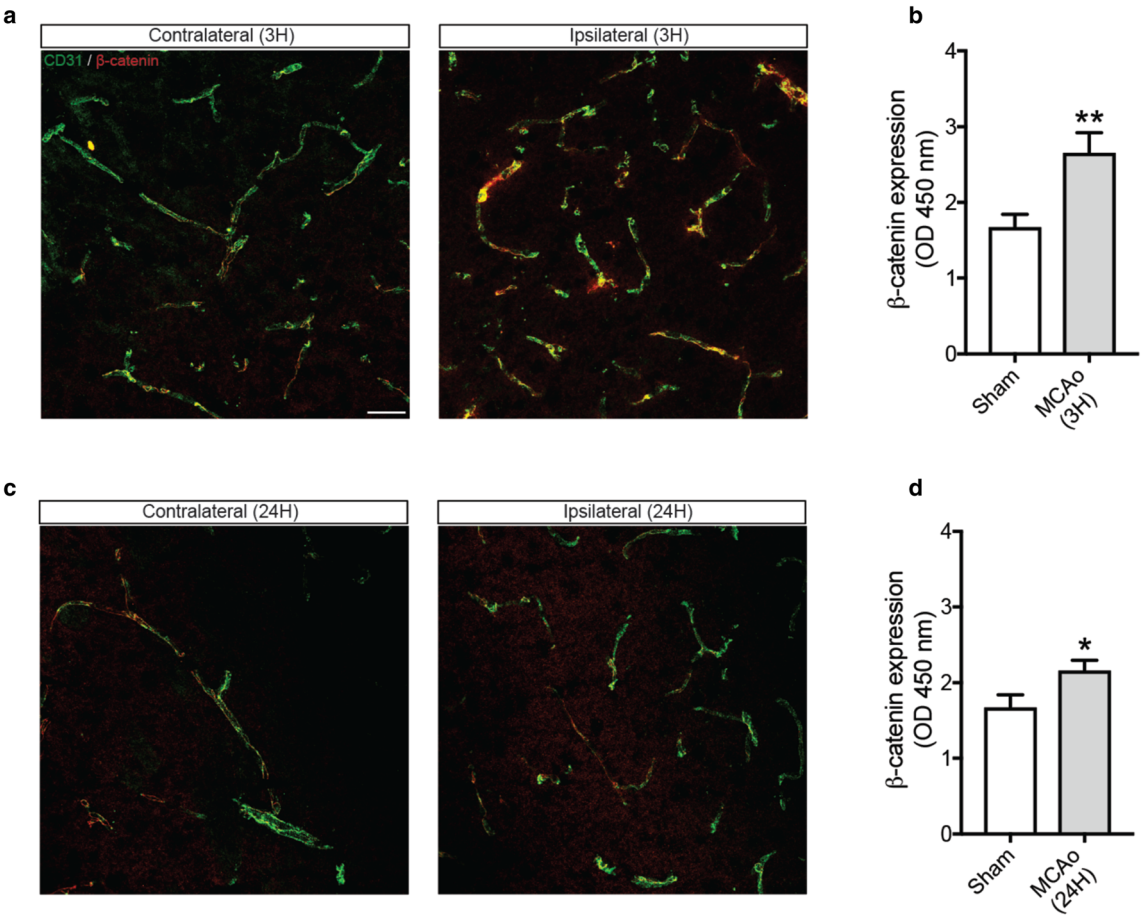

Fig. 1 Canonical Wnt pathway activity is detectable predominantly in brain endothelial cells and is induced upon ischemic stroke. Laser-scan confocal representative images of co-immunofluorescence staining for the active unphosphorylated form of β-catenin (Cy3; red) and $CD31^+$ (brain endothelial cell marker) (Alexa Fluor®488; green) show that active β-catenin co-localizes predominately with brain endothelial cells and is induced 3 h (**a**) and 24 h (**c**) after MCAo. **b** ELISA analysis shows that β-catenin levels strongly increase in isolated ischemic brain capillaries 3 h after MCAo. **d** ELISA analysis shows that β-catenin levels stay elevated in isolated ischemic brain capillaries 24 h after MCAo, but to a lesser extent in comparison to 3 h. MCAo, middle cerebral artery occlusion; ELISA, enzyme-linked immunosorbent assay. Data are mean ± SEM ($n = 6$ animals per group). The same sham group was used as control in **b** and **c** $*P < 0.05$/$**P < 0.01$ compared with sham group (standard two-tailed unpaired *t* tests). Laser-scan confocal images were acquired with a × 20 objective. Scale bar = 100 μm

limiting entry into the brain parenchyma. XAV939 systemic administration efficaciously deactivated the pathway in the ischemic brain endothelial cells, which was translated by reduced protein levels of β-catenin in isolated brain capillaries 24 h after MCAo induction (Fig. 2a). Importantly, brain infarct remained unchanged upon pathway deactivation 24 h after MCAo induction (Fig. 2b), while brain oedema increased (Fig. 2c), and the absolute number of vessels presenting perivascular bleeding, outlining localized hemorrhagic transformation, was exacerbated (Fig. 2d). These results indicate that pathway activity re-emerges as an intrinsic compensatory mechanism, which is required to preserve integrity of the disrupted BBB upon ischemic stroke.

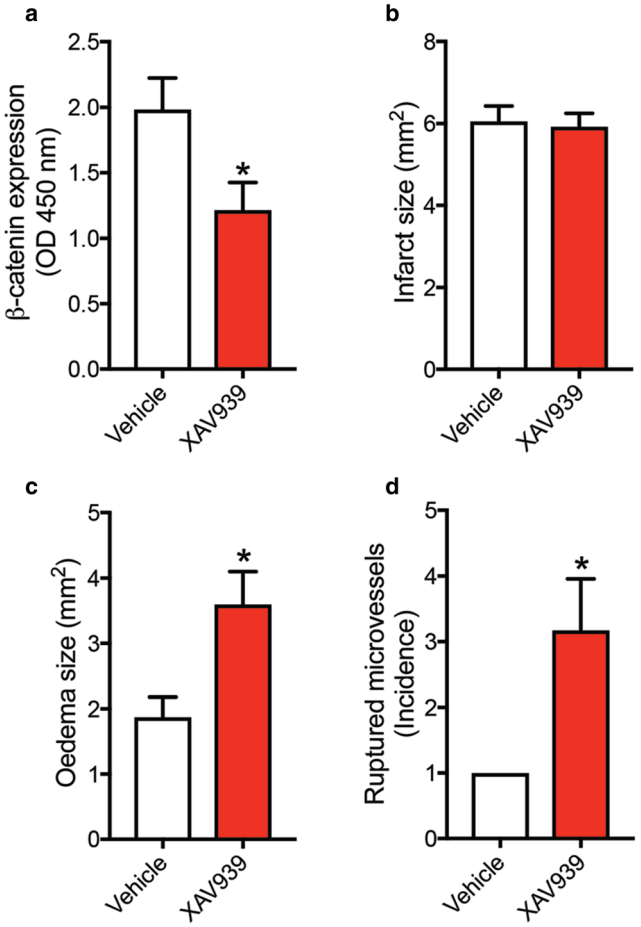

Fig. 2 Deactivation of the canonical Wnt pathway in brain endothelial early after ischemic stroke aggravates brain oedema and causes hemorrhagic transformation. **a** ELISA analysis demonstrates that XAV939 (40 mg/kg; intraperitoneal; one single dose immediately after MCAo) decreases β-catenin levels in isolated ischemic brain capillaries 24 h after MCAo. **b** Histochemistry analysis of cresyl violet staining shows that pathway early deactivation following systemic XAV939 injection does not influence brain infarct 24 h after MCAo. **c** Histochemistry analysis of cresyl violet staining indicates that pathway early pathway deactivation aggravates brain oedema 24 h after MCAo. **d** Histochemistry analysis of DAB staining shows that early pathway deactivation increases the incidence (ratio of ruptured microvessel number in experimental groups/mean ruptured microvessel number in vehicle-treated group) of spontaneous perivascular petechial bleeding (hemorrhagic transformation) 24 h after MCAo. ELISA, enzyme-linked immunosorbent assay; DAB, 3,3′-diaminobenzidine; MCAo, middle cerebral artery occlusion. Data are means ± SEM ($n = 6$ animals per group). *$P < 0.05$ compared with vehicle-treated group (standard two-tailed unpaired t test)

6-BIO Dose Dependently Activates the Pathway in Brain Endothelial Cells and Reverses OGD-Induced Endothelial Basal Permeability

6-BIO is a cell permeable non-toxic molecule, which has been shown to potently and specifically activate the canonical Wnt pathway in stem cells. To assess whether 6-BIO could efficaciously activate the pathway in brain endothelial cells, murine brain-derived endothelial cells (bEnd3) were used to perform dose-response experiments. 6-BIO activated the pathway in a dose-dependent manner, translated by an enhanced stabilization of β-catenin levels in the cytosol (Fig. 3a), and its subsequent translocation to the nucleus (Fig. 3b). Next functional studies were performed using bEnd3 exposed to OGD to mimic ischemic/reperfusion conditions in vitro. To investigate the impact of pathway activation on endothelial permeability, bEnd3 were cultured on a semi-permeable insert to form a monolayer of cells (Fig. 3c). OGD increased passage of the fluorescent tracer NaF across the bEnd3 monolayer, outlining an increased permeability, which was exacerbated by rtPA stimulation (Fig. 3c). However, 6-BIO treatment did not affect the passage of NaF across the bEnd3 monolayer (Fig. 3c). This observation could result from the severe damage caused by OGD and rtPA to the brain endothelial monolayer model, which does not allow dynamic re-establishment of firm inter-endothelial junctions upon disruption. Therefore, to better characterize the effects of 6-BIO on endothelial permeability, expression of PLVAP, an intra-endothelial cell-specific protein that mediates basal permeability via regulation of the formation of diaphragms, was analyzed. PLVAP is a direct target gene of the pathway and is repressed during BBB formation. Interestingly, OGD strongly induced PLVAP expression, which was further exacerbated by rtPA stimulation (Fig. 3d). On the other hand, 6-BIO potently repressed PLVAP protein expression associated to OGD with or without rtPA stimulation, reaching normoxic expression levels (Fig. 3d). 6-BIO induced caludin-5 protein expression in primary brain microvascular endothelial cells exposed to OGD (Fig. 3e), outlining 6-BIO potency in inducing BBB-specific markers. These results indicate that 6-BIO activates the pathway in brain endothelial cells and reduces OGD-exacerbated basal endothelial permeability via regulation of specific intra-endothelial permeability mechanisms.

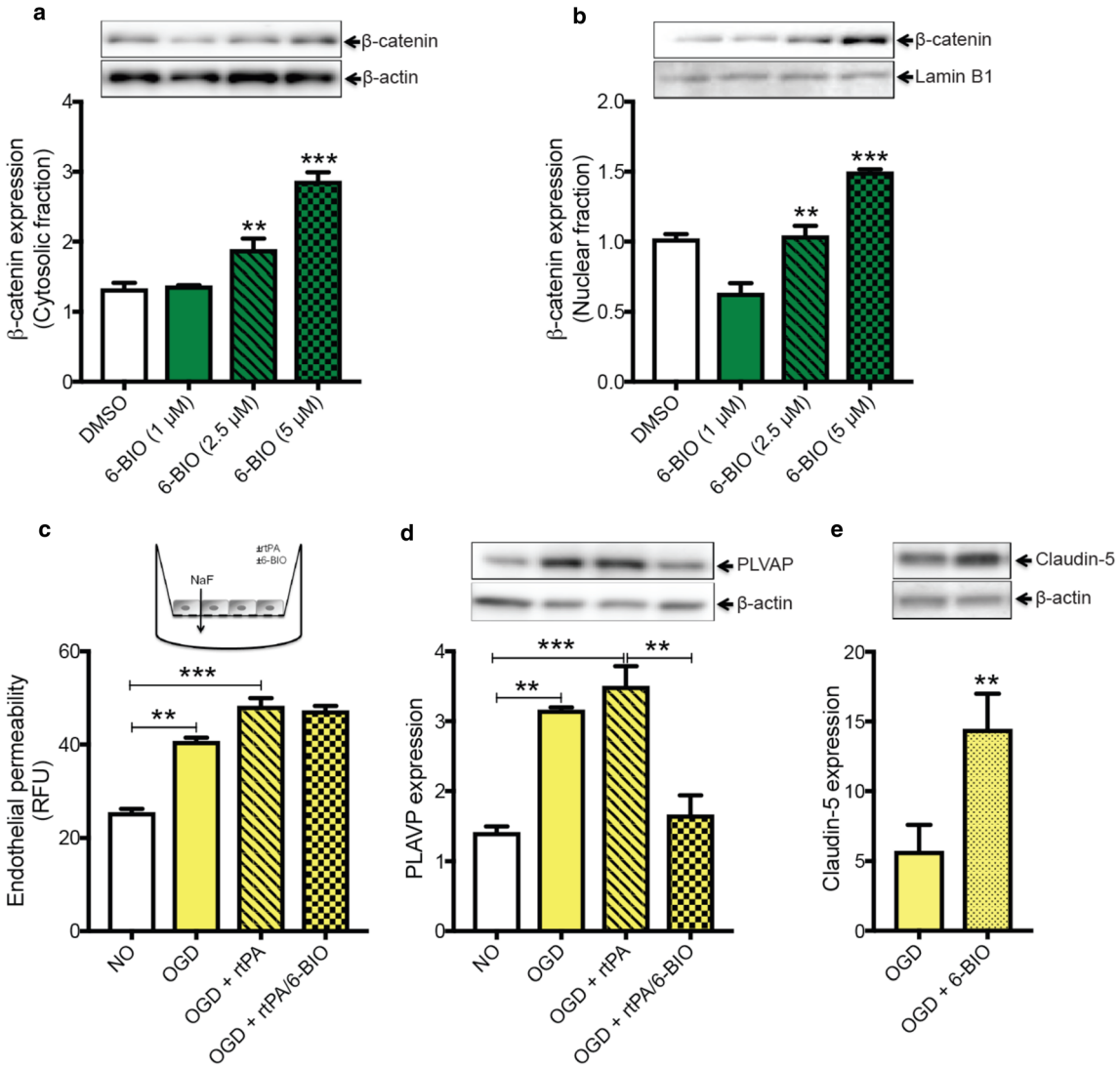

Fig. 3 6-BIO efficaciously activates the canonical Wnt pathway in brain endothelial cells and decreases the OGD-induced basal permeability. **a** Western blot analysis shows that 6-BIO increases β-catenin protein expression in the cytosol of bEnd3 cells in a dose-dependent manner. **b** Western blot analysis shows that 6-BIO ameliorates β-catenin translocation to the nucleus of bEnd3 cells in a dose-dependent manner. **c** Paracellular permeability assay indicates that NaF efflux through the monolayer bEnd3 cells increases following exposure to OGD, and is exacerbated upon delayed rtPA stimulation (20 μg/ml; 6 h after OGD). Paracellular permeability was assessed using NaF. **d** Western blot analysis shows that the OGD-induced PLVAP protein expression further increases following delayed stimulation with rtPA, but is repressed upon canonical Wnt pathway activation following stimulation with 6-BIO (5 μM; 3 and 6 h after OGD). **e** Western blot analysis shows that 6-BIO treatment potently increases claudin-5 expression in primary brain microvascular endothelial cells exposed to OGD. 6-BIO, 6-bromoindirubin-3′-oxime; bEnd3, brain endothelial cells; DMSO, dimethyl sulfoxide; NaF, sodium fluorescein; OGD, oxygen and glucose deprivation; NO, normoxia; rtPA, recombinant tissue plasminogen activator; PLVAP, plasmalemma vesicle associated protein; RFU, relative fluorescent unit. Data are mean ± SEM ($n = 3$ independent experiments per condition). $^{**}P < 0.01$/$^{***}P < 0.001$ compared with either DMSO-treated, or different NO and OGD conditions (one-way analysis of variance (ANOVA) followed by Tukey's post hoc test)

Pathway Activation Ameliorates BBB Tightness and Reduces Incidence of rtPA-Induced Perivascular Bleeding

Next, the effects of canonical Wnt pathway activation following 6-BIO treatment on brain injury and BBB integrity were evaluated in vivo. 6-BIO was administrated systemically to allow optimal accumulation within the leaky ischemic vasculature as mentioned before. A first dose was administered within the therapeutic window of rtPA and a second dose was administered beyond it. This treatment strategy aims to maximize the effect of pathway activation in protecting the BBB at early and delayed stages. Noticeably, neither delayed rtPA administration nor 6-BIO treatment influenced brain infarct (Fig. 4a, c). Nonetheless, 6-BIO reduced the deleterious effects of delayed rtPA administration on brain oedema

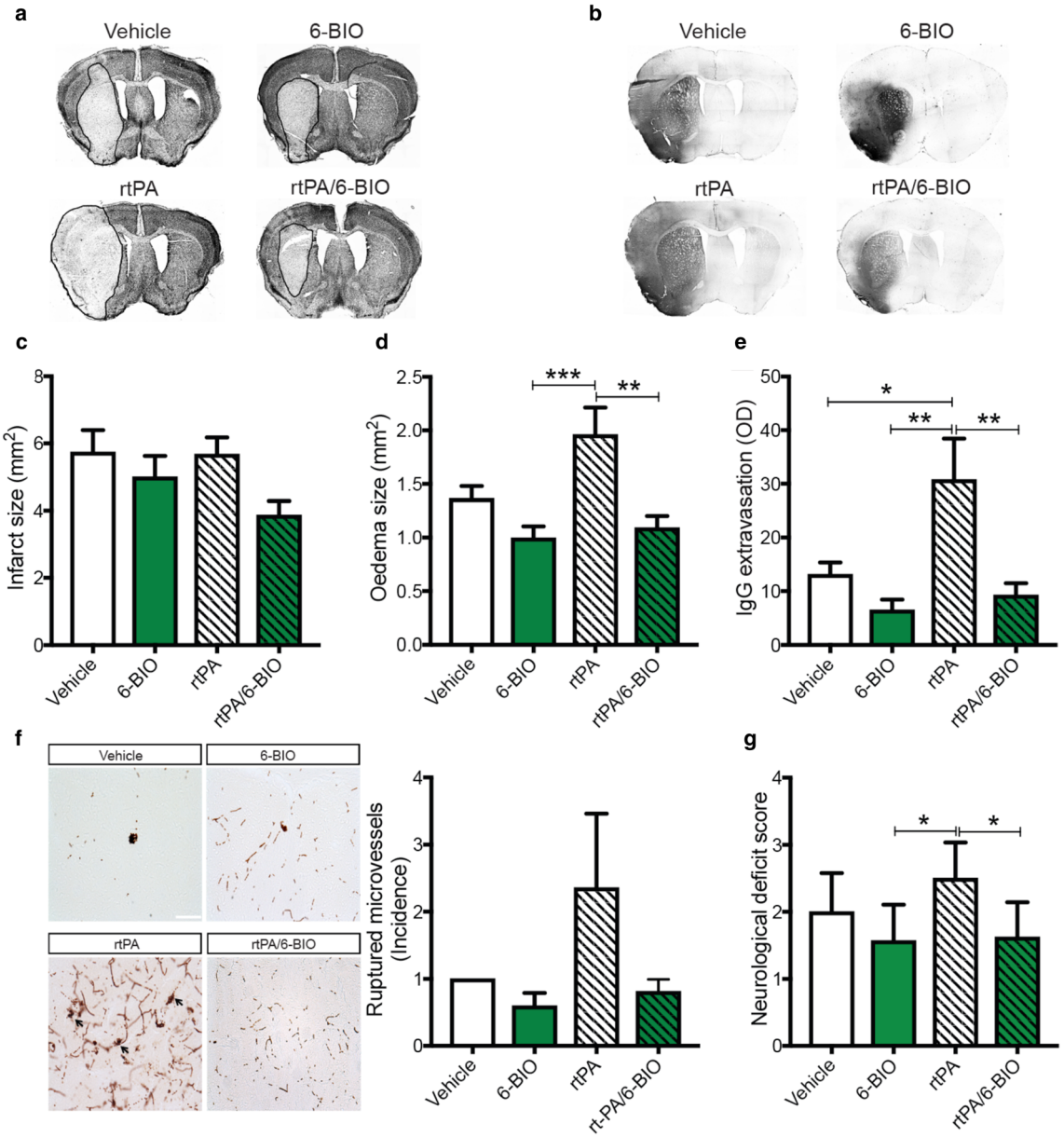

Fig. 4 6-BIO attenuates BBB breakdown and reduces the incidence hemorrhagic transformation associated to delayed rtPA administration after stroke. **a**, **c** Histochemistry analysis of cresyl violet staining shows that neither delayed rtPA administration (10 mg/kg; intravenous; 6 h after MCAo) nor 6-BIO treatment (1 mg/kg; intraperitoneal; 2 doses 3 and 6 h after MCAo) affect brain infarct 24 h after MCAo. **a**, **d** Histochemistry analysis of Cresyl violet staining shows that systemic treatment with 6-BIO attenuates brain oedema aggravation associated to delayed rtPA administration 24 h after MCAo. **b**, **e** Immunohistochemical analysis of DAB staining shows that systemic treatment with 6-BIO reduces exacerbated IgG extravasation into the brain parenchyma associated to delayed rtPA administration 24 h after MCAo. **f** Histochemistry analysis of DAB staining shows that systemic treatment with 6-BIO tends to decrease the incidence (ratio of ruptured microvessel number in each different experimental groups/mean of ruptured microvessel number in vehicle-treated group) of rtPA-induced perivascular petechial bleeding increases (hemorrhagic transformation) 24 h after MCAo. **g** The neurological score test indicates that 6-BIO attenuated exacerbation of the neurological deficits associated to delayed rtPA administration in mice 24 h after MCAo. 6-BIO did not influence neurological deficits of vehicle-treated mice. MCAo, middle cerebral artery occlusion; BBB, blood-brain barrier; 6-BIO, 6-bromoindirubin-3′-oxime; DMSO, dimethyl sulfoxide; rtPA, recombinant tissue plasminogen activator; DAB, 3,3′-diaminobenzidine. Data are mean ± SEM ($n = 6$–8 animals per group). $^{*}P < 0.05$/$^{**}P < 0.01$/$^{***}P < 0.001$ compared with vehicle-treated and different conditions (one-way analysis of variance (ANOVA) followed by Tukey's post hoc test)

(Fig. 4a, d), IgG extravasation (Fig. 4b, e), and the incidence of microvessel presenting perivascular bleeding (Fig. 4f), 24 h after MCAo induction. Column statistics (mean ± SEM) of the number of ruptured microvessels showed (vehicle, 9.875 ± 4.244; 6-BIO, 5.714 ± 2.598; rtPA, 26.5 ± 13.32; rtPA/6-BIO, 8.25 ± 2.297), outlining an increase in the absolute number of vessels presenting perivascular bleeding. 6-BIO attenuated exacerbation of the neurological deficits associated to

delayed rtPA administration in mice 24 h after MCAo induction (Fig. 4g). 6-BIO did not influence neurological deficits in vehicle-treated mice. The findings suggest that pathway activation by 6-BIO limited BBB breakdown caused by delayed administration of rtPA—without directly acting as neuroprotectant—and consequently reduced the deleterious effects of delayed rtPA administration on neurological functions. Importantly, MMP-2/9 gelatinase activity remained unchanged among the rtPA- and rtPA/6-BIO-treated groups (0.5188 ± 0.009478; 0.519 ± 0.03247, respectively), suggesting that the 6-BIO preserved BBB integrity without affecting rtPA proteolytic activity, and thus thrombolytic efficacy. These results clearly indicate that pathway activation via systemic administration of 6-BIO after ischemic stroke significantly extends the therapeutic window of rtPA by specifically attenuating BBB breakdown.

6-BIO Administration Does Not Influence Ischemic Stroke–Associated Neuronal Injury, Angiogenesis, and Inflammation

Structural assessment of brain injury does not exclude direct neuroprotective effect of 6-BIO on the cellular level. Moreover, blood-derived rtPA has been shown to cross the disrupted BBB, and is associated with neurotoxicity that affects vulnerable brain structures [29, 30]. As such, neuronal degeneration associated to rtPA was assessed in the striatum and overlaying cortex, which are brain structures directly damaged by the MCAo model used in this study, as well as in the hippocampus, which is a vulnerable brain structure indirectly damaged by MCAo. Interestingly, delayed rtPA administration and 6-BIO treatment did not influence neuronal degeneration (FJB^+ cells) in the striatum (Fig. 5a), and the cortex (Fig. 5b), indicating that 6-BIO does not provide direct protective effects to severely damaged structures. Importantly, 6-BIO attenuated the effect of delayed rtPA administration on neuronal degeneration in the hippocampus without influencing the damage associated to ischemic stroke alone (Fig. 5c), as 6-BIO did not reduce neuronal degeneration when compared to vehicle-treated animals. This would suggest that 6-BIO indirectly protected the vulnerable neurons in the hippocampus, most probably via BBB preservation, which reduces rtPA-exaggerated accumulation in the ischemic brain. Indeed, 6-BIO administration attenuated the excessive accumulation of rtPA in the ischemic brain (Fig. 5d). Ischemic stroke triggers angiogenic and inflammatory responses, and some reports suggest that the canonical Wnt pathway is implicated in regulating these responses. As such, neovascularization and activation of microglial cells were investigated. Delayed rtPA administration and 6-BIO treatment did not affect microvasculature density (Fig. 5e), and the turnover of microglial cells (Fig. 5f) 24 h after MCAo induction. These results indicate that 6-BIO does not influence the angiogenic and inflammatory responses in the acute phase of ischemic stroke.

6-BIO Systemic Administration Induces and Stabilizes Pathway Activity Specifically in Brain Microvasculature

Afterwards, the mechanisms underlying the vascular effects of 6-BIO were evaluated. Delayed rtPA administration did not influence the expression levels of β-catenin (Fig. 6a, b). However, 6-BIO treatment increased β-catenin microvascular expression in the ischemic and non-ischemic hemispheres (Fig. 6a, b), outlining a potent efficacy in activating the pathway in brain endothelial cells. No signal was detected in the parenchyma, suggesting that pathway activity is predominantly induced in brain microvasculature. Strikingly, delayed rtPA administration was associated to a reduced density of β-catenin$^+$ microvascular structures, translated by discontinuous β-catenin expression, thus outlining instable pathway activity (Fig. 6a, c). These effects were completely reversed following treatment with 6-BIO, which increased the density of β-catenin$^+$ microvascular structures, translated by continuous β-catenin expression, thus outlining a stable pathway activity (Fig. 6a, c). These results suggest that systemic administration of 6-BIO potently activates the pathway in the microvasculature.

Pathway Activation Attenuates Tight Junction Disruption and Basal Endothelial Permeability Associated to Delayed rtPA Administration

Finally, the mechanisms underlying the effects of canonical Wnt pathway activation on BBB integrity were investigated in vivo. For this purpose, expression of the tight junction protein claudin-3, a direct target gene of the pathway, and fragmentation of the claudin-3$^+$ microvascular structures, which translates disruption of claudin-3 assembly between adjacent endothelial cells, were first evaluated. Importantly, delayed rtPA administration reduced claudin-3 microvascular expression in the ischemic and non-ischemic hemispheres (Fig. 7a, b). Pathway activation increased claudin-3 microvascular expression (Fig. 7a, b). Furthermore, delayed rtPA administration increased the fragmentation of claudin-3$^+$ microvascular structures in the ischemic hemisphere, which was exacerbated in the ischemic hemisphere (Fig. 7a, c), suggesting that delayed rtPA administration deregulates tight junctions even in the intact brain tissue, an effect that was amplified in the ischemic tissue. Importantly, fragmentation of claudin-3$^+$ microvascular structures was totally

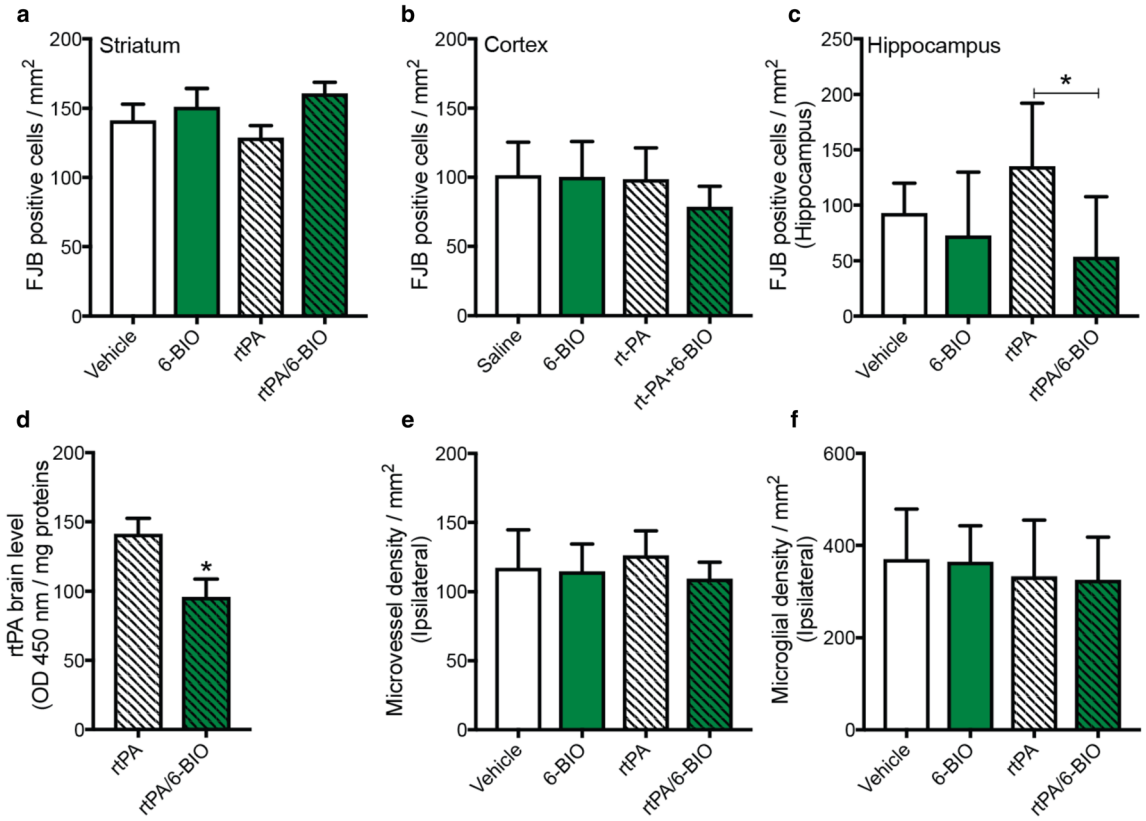

Fig. 5 6-BIO attenuates rtPA-associated neuronal degeneration in the hippocampus without influencing angiogenesis and inflammation after ischemic stroke. **a** FJB analysis outlines no difference among all groups in the number of degenerating neurons in the striatum of the ipsilateral hemisphere 24 h after MCAo. **b** FJB analysis outlines no difference among all groups in the number of degenerating neurons in the cortex of the ipsilateral hemisphere 24 h after MCAo. **c** FJB analysis outlines an exacerbation of neuronal degeneration in the hippocampus following delayed rtPA administration (10 mg/kg; intravenous; 6 h after MCAo), in the ipsilateral hemisphere 24 h after MCAo, and effect that is attenuated by 6-BIO treatment (1 mg/kg; intraperitoneal; 2 doses 3 and 6 h after MCAo). **d** ELISA assay shows that 6-BIO reduces the entry of blood-derived rtPA into the ipsilateral hemisphere 24 h after MCAo brain. **e** Immunofluorescence analysis for CD31 (endothelial cell marker) quantification shows that neither 6-BIO treatment nor delayed rtPA administration, alone or combined, affected brain microvasculature density in the ipsilateral hemisphere 24 h after MCAo. **f** Immunofluorescence analysis for Iba1 (microglial cell marker) shows that neither 6-BIO nor rtPA, alone or combined, influenced the density of microglial cells in the ipsilateral hemisphere 24 h after MCAo. Sections representing the striatum and the overlaying cortex per animal's brain were used for immunofluorescence staining and subsequent quantification. MCAo, middle cerebral artery occlusion; FJB, fluoro-jade B; 6-BIO, 6-bromoindirubin-3′-oxime; rtPA, recombinant tissue plasminogen activator; Iba1, ionized calcium binding adaptor molecule-1. Data are mean ± SEM ($n = 6–8$ animals per group). One-way analysis of variance (ANOVA) followed by Tukey's post hoc test was used to perform statistical analysis

abolished in both hemispheres following pathway activation (Fig. 7a, c). Next, endothelial basal permeability was evaluated by analyzing the vesicular accumulation of HRP^+ inclusions in endothelial cells (translating luminal permeability) and astrocytic processes ensheathing the basal membrane of capillaries (translating basal permeability). Delayed rtPA administration did not affect the number of circulatory HRP^+ inclusions in ischemic brain endothelial cells, while 6-BIO treatment tended to slightly reduce the number of inclusions without reaching statistical significance (Fig. 8a, b). In contrast, delayed rtPA administration potently exacerbated the number of circulatory HRP^+ inclusions in astrocytic endfeet, which was attenuated by 6-BIO treatment (Fig. 8a, c). These overall results show that pathway activation attenuates BBB breakdown by promoting formation and stabilization of the tight junctions, and reducing basal endothelial permeability.

Discussion

Our study highlights a key role of canonical Wnt pathway in preserving and maintaining BBB structural and functional integrity after ischemic stroke. The findings highlight pathway's potential as a promising target for the development of novel adjuvant interventions that aim at ameliorating rtPA therapy. Using in vivo approaches, we found that β-catenin expression, which translates pathway activation, is induced predominately in brain endothelial cells early after ischemic stroke. Early pharmacological deactivation of the pathway using XAV939 exacerbated

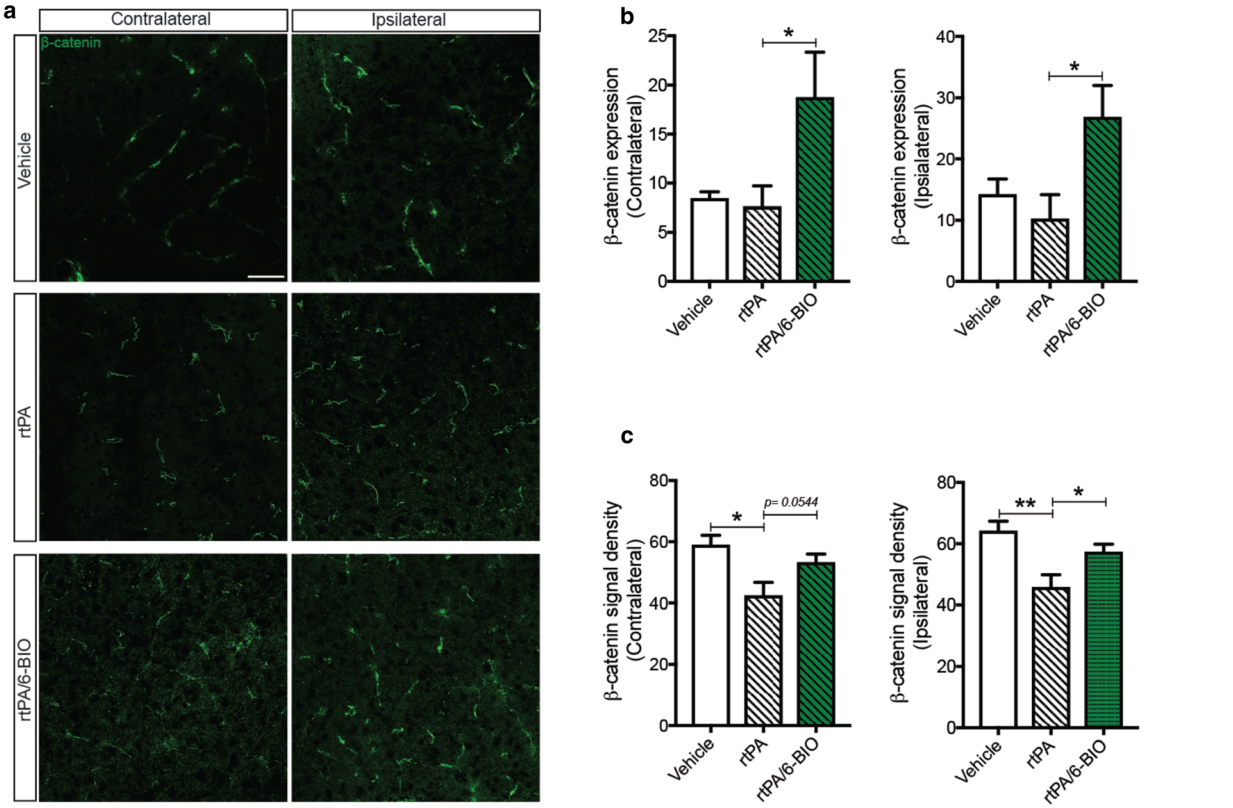

Fig. 6 Delayed rtPA administration impairs canonical Wnt pathway activity in brain endothelial cells, which is rescued by 6-BIO systemic treatment. **a** Laser-scan confocal representative images of immunofluorescence staining for the active unphosphorylated form of β-catenin in the brain 24 h after MCAo. **b** Analysis of immunofluorescence staining shows that systemic administration of 6-BIO (1 mg/kg; intraperitoneal; 2 doses 3 and 6 h after MCAo) increases β-catenin expression (number of β-catenin$^+$ vessels/mm^2) that is reduced following the delayed administration of rtPA (10 mg/kg; intravenous; 6 h after MCAo) in the contralateral and ipsilateral hemisphere 24 h after MCAo. **c** Analysis of immunofluorescence staining shows that systemic administration of 6-BIO restored β-catenin vascular density (length of β-catenin vessels/mm^2) that is impaired following the delayed administration of rtPA in the ipsilateral hemisphere 24 h after MCAo. MCAo, middle cerebral artery occlusion; 6-BIO, 6-bromoindirubin-3′-oxime; rtPA, recombinant tissue plasminogen activator. Data are mean ± SEM (n = 6–8 animals per group). *P < 0.05/**P < 0.01 compared with vehicle-treated and different conditions (standard two-tailed unpaired t test). Laser-scan confocal images were acquired with a × 20 objective. Scale bar = 150 μm

BBB breakdown, and increased perivascular bleeding, outlining a hemorrhagic transformation, 24 h after ischemic stroke. Using cell-based assays, we found that 6-BIO, a potent reversible GSK3β inhibitor efficaciously activated the pathway in brain endothelial cells via stabilization of β-catenin in the cytosol and stimulation of its subsequent translocation to the nucleus. Delayed incubation of brain endothelial cells exposed to ischemic-like conditions with rtPA increased PLVAP expression, which was attenuated by 6-BIO. Furthermore, our in vivo investigations showed that systemic treatment of mice with 6-BIO efficiently activated the pathway in brain endothelial cells 24 h after ischemic stroke. Pathway activation attenuated the deleterious effects of rtPA, which was administered 6 h after ischemic stroke onset, on BBB breakdown and hemorrhagic transformation. Protection of BBB structural and functional characteristics associated to pathway activation was achieved through the attenuation of tight junction disruption and reduction of endothelial basal permeability. BBB presentation upon pathway activation attenuated exacerbation of the neurological deficit associated to delayed rtPA administration.

The BBB constitutes a highly selective structure that prevents para-endothelial diffusion of small blood-borne molecules due to the presence of tight junctions, and restricts the trans-endothelial passage of large blood-borne molecules due to lack of fenestrations that mediate basal endothelial permeability [31]. BBB characteristics are orchestrated by canonical Wnt pathway during ontogeny [14]. In brain endothelial cells, β-catenin stabilization and subsequent translocation to the nucleus activate the LEF/TCF transcription factor, specifically regulating expression of major BBB-specific target genes [5, 14]. The β-catenin-LEF/TCF signaling induces expression of the tight junction protein claudin-3, and represses expression of PLVAP, which promotes formation of permeable fenestrae (i.e., diaphragms) in endothelial cells [14]. Although pathway activity is reduced in brain endothelial cells upon barrier formation and maturity in the adult brain, it remains essential to

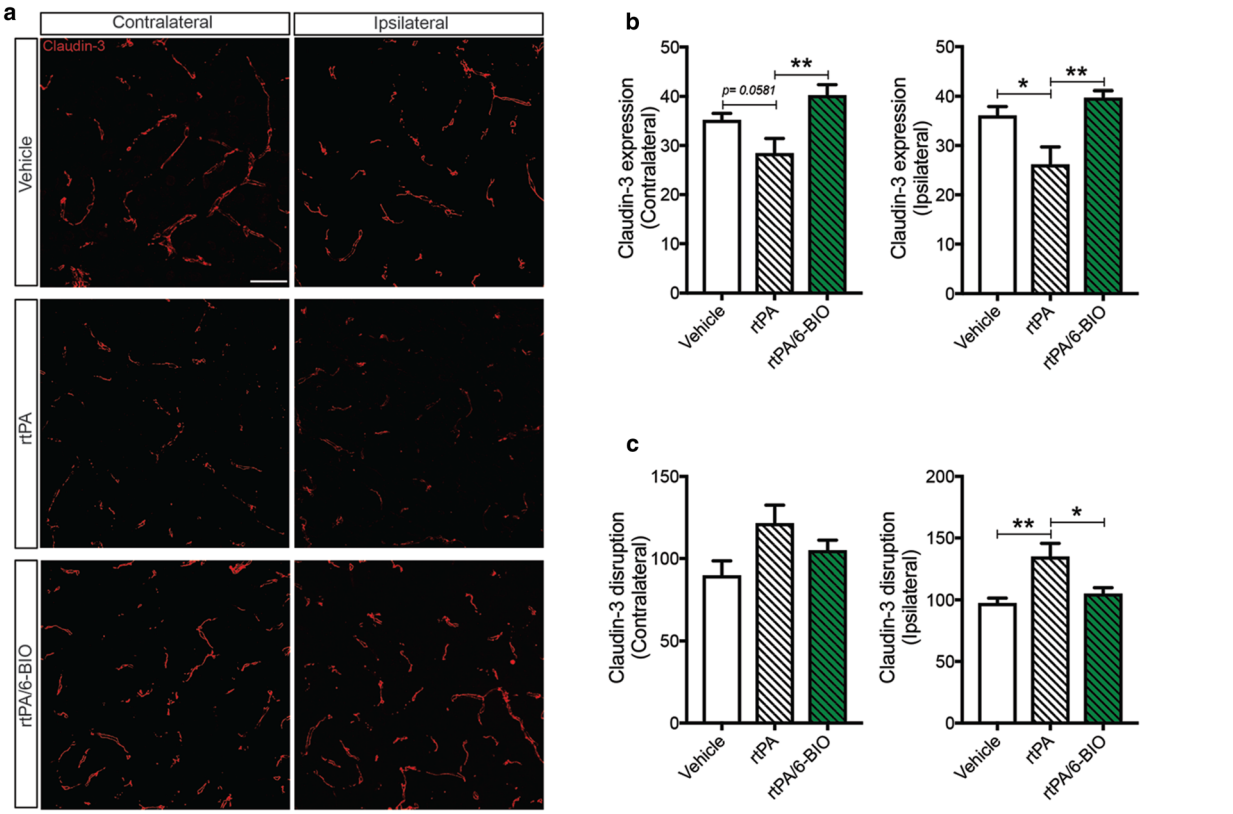

Fig. 7 6-BIO systemic administration attenuates tight junction disruption associated to delayed rtPA administration. **a** Laser-scan confocal representative images of immunofluorescence staining for claudin-3, which is a direct target for β-catenin/LEF/TCF signaling, in the brain 24 h after MCAo. **b** Analysis of immunofluorescence staining shows that systemic administration of 6-BIO (1 mg/kg; intraperitoneal; 2 doses 3 and 6 h after MCAo) increases claudin-3 expression (number of claudin-3$^+$ vessels/mm^2) that is reduced following the delayed administration of rtPA (10 mg/kg; intravenous; 6 h after MCAo) in the ipsilateral hemisphere 24 h after MCAo. **c** Analysis of immunofluorescence staining shows that systemic administration of 6-BIO attenuates claudin-3 disruption (length of β-catenin vessels/mm^2) that is increased following the delayed administration of rtPA in the ipsilateral hemisphere 24 h after MCAo. MCAo, middle cerebral artery occlusion; 6-BIO, 6-bromoindirubin-3′-oxime; rtPA, recombinant tissue plasminogen activator. Data are mean ± SEM ($n = 6$–8 animals per group). $^*P < 0.05$/$^{**}P < 0.01$ compared with vehicle-treated and different conditions (standard two-tailed unpaired t test). Laser-scan confocal images were acquired with a × 20 objective. Scale bar = 150 μm

maintain BBB characteristics across the lifespan [15]. Moreover, β-catenin depletion in brain endothelial cells causes diffuse spontaneous perivascular petechial hemorrhages in the normal brain [15]. Active β-catenin is barely detectable in brain endothelial cells under physiological conditions. However, pathway activity re-remerges under pathological conditions associated to BBB breakdown, such as multiple sclerosis (MS), outlining a possible intrinsic compensatory mechanism aiming to restore BBB function [16]. How the pathway is regulated upon ischemic stroke in brain endothelial cells, and whether its activity affects BBB breakdown in the acute phase remains totally elusive. Here, we showed that active β-catenin levels are induced predominately in brain endothelial cells very early after ischemic stroke. Importantly, active β-catenin levels were below the detection threshold in brain parenchymal cells. Previous brain-mapping studies have outlined recapitulation of embryonic organizational patterns upon ischemic stroke, and that recovery constitutes a return to adult patterns [32]. Due to its pivotal role in orchestrating BBB formation and maturation, canonical Wnt pathway re-emergence could constitute a facet of embryonic organizational pattern recapitulation. Reduction of β-catenin levels immediately upon ischemic stroke using pharmacological approaches increased brain oedema and augmented spontaneous perivascular petechial bleeding. These results are in line with recent findings reporting low β-catenin levels specifically in brain endothelial cells located near bleeding sites in the brain of hemorrhagic stroke patients [15].

Currently, rtPA-induced thrombolysis remains the gold standard therapy for acute ischemic stroke [9]. rtPA should be administered within a therapeutic window of 4.5 h after stroke onset [10]. Unfortunately, many patients do not qualify for rtPA, as they present for evaluation 4.5 h after onset [9]. rtPA administration beyond the 4.5 h after onset has serious life-threatening side effects, mainly hemorrhagic transformation, which constitutes a major cause of morbidity and mortality in stroke patients [33]. Furthermore, even patients treated with rtPA within the established therapeutic window are at

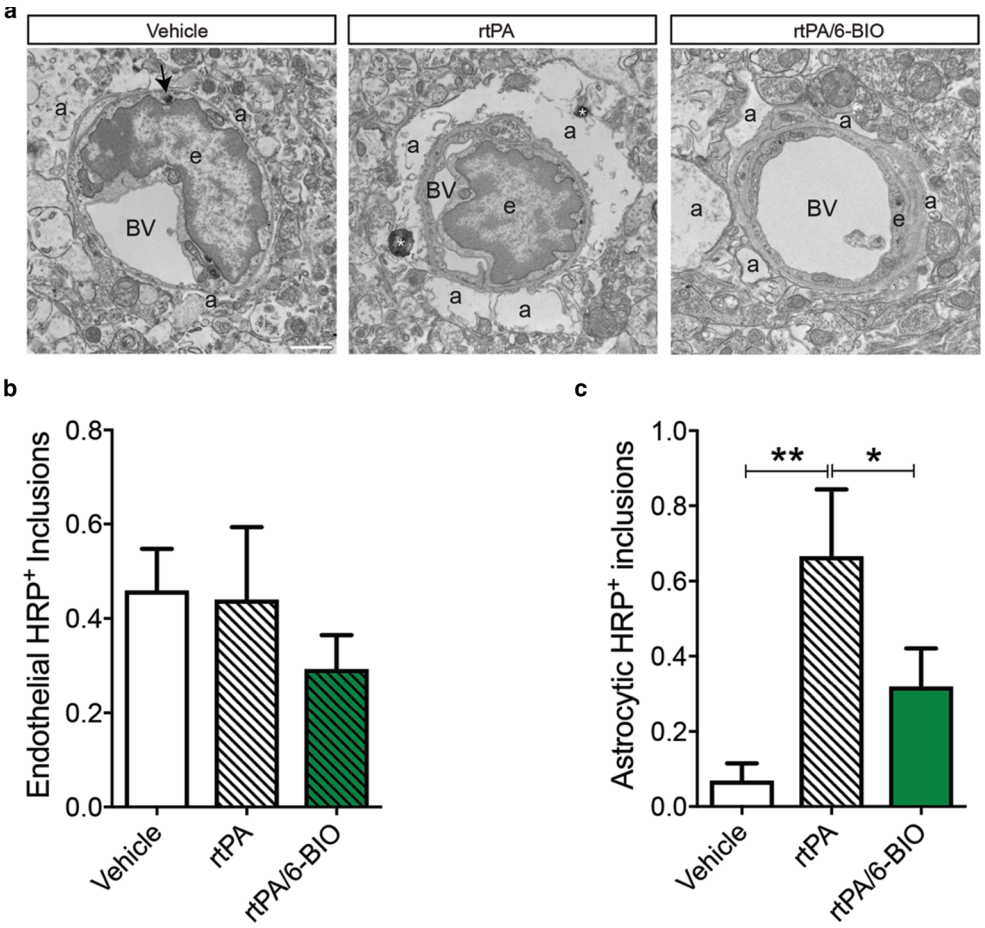

Fig. 8 6-BIO systemic administration recovers basal endothelial permeability after delayed rtPA administration. **a** TEM representative images illustrating HRP inclusions in endothelial cells (e) and astrocytic endfeet (a). **b** TEM analysis shows that neither delayed rtPA administration nor 6-BIO treatment influenced the number of HRP^+ inclusions within endothelial cells of capillaries. **c** TEM analysis shows that delayed rtPA administration significantly increases the number HRP^+ inclusions within astrocytic endfeets juxtaposing the basal membrane of capillaries. HRP, horseradish peroxidase 6-BIO, 6-bromoindirubin-3′-oxime; rtPA, recombinant tissue plasminogen activator; BV, blood vessel lumen. Data are mean ± SEM (n = 120 vessels per animal). $^*P < 0.05$/$^{**}P < 0.01$ compared with rtPA-treated condition (Kruskal-Wallis one-way analysis of variance (ANOVA) followed by the Dunn post hoc test). TEM images were acquired at × 4800. Scale bar = 1 μm

elevated risk of hemorrhagic transformation [34]. Limiting the deleterious effects of rtPA and extending its therapeutic window will have major clinical impact via reduction of morbidity and mortality in patients, and this significantly increases the number of patients eligible for thrombolysis [33]. The deleterious effects of rtPA are essentially caused by exacerbation of BBB breakdown associated to MMPs activation [9]. Strategies to inhibit MMPs were successful in reducing brain oedema, and rtPA-associated hemorrhage [9]. However, MMPs inhibition could alter post-stroke endogenous restorative processes [35]. Therefore, developing novel adjuvant interventions that specifically limit rtPA-associated BBB breakdown without affecting thrombolysis or altering neurorestoration is the challenge to be met. In the recent years, several strategies were assessed in pre-clinical studies, such as administration of statins, kinase inhibitors (e.g., rho kinase inhibitors), G protein–coupled receptor (GPCR) antagonists (e.g., angiotensin II inhibitors), immunomodulatory molecules (e.g., granulocyte colony-stimulating factor (G-CSF)), metabolic modulators (e.g., optimized human apyrase), and stem cell transplantation (e.g., endothelial progenitor cells (EPCs) [33, 36]. Thought interesting, these strategies do not target BBB-specific mechanisms, and the reported BBB preservation is often secondary to neuroprotection. In our study, we hypothesized that pathway activation in brain endothelial cells would allow BBB preservation by targeting BBB-specific mechanisms.

BBB breakdown after ischemic stroke is characterized by disruption of the tight junctions [5], and is associated to up-regulation of PLVAP expression [37, 38]. Our cell-based investigations showed that treating brain endothelial cells with 6-BIO, a pathway activator that acts by inhibiting GSK3β, stabilized β-catenin in the cytosol and promoted its subsequent translation to the nucleus. Importantly, we found that OGD increased para-endothelial permeability and induced PLVAP expression, which was accentuated upon delayed rtPA stimulation. Stabilization of β-catenin repressed rtPA-induced PLVAP expression. Our findings suggest that delayed rtPA exacerbated trans-endothelial permeability associated to ischemic-like conditions, an effect that was attenuated by 6-BIO-induced pathway activation. 6-BIO did not restore the para-endothelial cellular permeability in vitro, which can be explained by the fact that cell loss could not be rapidly compensated in a monolayer of cells in vitro to re-establish tight inter-endothelial contacts. Our in vivo approaches showed that treating mice with 6-BIO decreased brain oedema, reduced IgG extravasation, and diminished the incidence of perivascular petechial bleeding 24 h after MCAo induction.

Structural and cellular neuronal injuries were not affected by 6-BIO treatment 24 h after MCAo induction, thus excluding direct neuroprotective effects. It was worthy to note that neuronal degeneration was attenuated in the hippocampus, a brain structure that is not directly affected by occlusion of the MCA, but highly vulnerable to hypoxia/ischemia [39]. Focal cerebral ischemia has been shown to cause tPA-induced neurotoxicity in the hippocampus [39]. Our results indicate that rtPA accumulates in the brain due to BBB breakdown, thus presumably exacerbating neurotoxicity in the hippocampus. It is conceivable to speculate that BBB preservation attenuated neurotoxicity in the hippocampus by decreasing rtPA accumulation. Preservation of the BBB upon canonical Wnt pathway activation reduced neurological following rtPA-delayed administration, without influencing neurological deficits in vehicle-treated mice. Furthermore, 6-BIO treatment did not affect the angiogenic and inflammatory responses 24 h after MCAo induction. The protective effects of 6-BIO treatment on BBB integrity were accompanied by elevated levels of active β-catenin specifically in brain endothelial cells of both ipsilateral and contralateral hemispheres, and by an increased density of β-catenin$^+$ microvasculature. Importantly, delayed rtPA administration did not affect β-catenin expression but rather impaired density of β-catenin in the microvasculature, outlining an impact of rtPA on β-catenin disruption in brain endothelial cells. To elucidate how pathway activation via 6-BIO treatment mediated BBB preservation, we investigated claudin-3 turnover and endothelial basal permeability associated to the formation of endothelial fenestral diaphragms that facilitate the passage of inclusions from the luminal side towards the perivascular space and brain parenchyma. Both mechanisms are direct targets of the canonical Wnt pathway. Delayed rtPA administration reduced claudin-3 expression in both ipsilateral and contralateral hemispheres, and potentiated fragmentation of claudin-3$^+$ microvasculature in the ipsilateral hemisphere, outlining an impaired assembly of claudin-3 in ischemic brain endothelium. β-catenin stabilization via 6-BIO treatment rescued claudin-3 expression, and attenuated fragmentation of claudin-3$^+$ microvasculature. Furthermore, delayed rtPA administration significantly increased the transfer of circulatory HRP from the endothelial cells through the basal membrane towards the astrocytic endfeet, outlining exacerbated basal endothelial permeability. This observation indicates that 6-BIO potently attenuated the effects of delayed rtPA administration on basal endothelial permeability. These findings indicate that the approach we have applied modulated BBB-specific mechanisms. In a recent study, the effect of GSK3β inhibition on rtPA was evaluated in rats [40]. However, rtPA was administered within the established therapeutic window, 4 h after stroke onset, and the strategy used to inhibit GSK3β was potently neuroprotective, thereby making it difficult to interpret data especially in regard to extension of the time window. In our study, we chose the 6-h time window, as it has been reported that such expansion will have substantial impact in clinics [41]. To our knowledge, our study is the first to evaluate the impact of canonical Wnt pathway activation on delayed rtPA administration.

Collectively, our findings unraveled a new role of the canonical Wnt pathway in preserving and maintaining BBB characteristics after ischemic stroke. Pathway activity re-emerges early upon ischemic stroke predominantly in brain endothelial cells, an intrinsic process that seems to be essential to limit BBB breakdown. Our findings suggest that pathway activation using 6-BIO constitutes a promising strategy to limit the deleterious effects of rtPA and extending its therapeutic window in acute ischemic stroke.

Acknowledgements We would like to thank Mrs. Revathy Guruswamy for performing some of the MCAo surgeries, Dr. Nathalie Vernoux for preparing the brain samples for TEM, and Mrs. Julie-Christine Lévesque at the Bio-Imaging Platform of CRCHU de Québec for technical assistance.

Funding Information This study was financially supported by grants from the Natural Sciences and Engineering Research Council of Canada (NSERC), Heart and Stroke Foundation of Canada (HSFC), and *Fonds de recherche du Québec - Santé (FRQS)* (all to AEA). NJL was supported by a scholarship from the NSERC, and a scholarship from the *Fondation du CHU de Québec*. KP was supported by a scholarship from the *Fondation du CHU de Québec*. MET is a Canada Research Chair (Tier 2) in *Neuroimmune Plasticity in Health and Therapy.*

Compliance with Ethical Standards

Animal experiments were performed according to the Canadian Council on Animal Care guidelines, as administered by the Université Laval Animal Welfare Committee.

Conflict of Interest The authors declare that they have no conflict of interest.

Publisher's Note Springer Nature remains neutral with regard to jurisdictional claims in published maps and institutional affiliations.

References

1. Dirnagl U (2012) Pathobiology of injury after stroke: the neurovascular unit and beyond. Ann N Y Acad Sci 1268:21–25. https://doi.org/10.1111/j.1749-6632.2012.06691.x
2. Hanley DF, Awad IA, Vespa PM, Martin NA, Zuccarello M (2013) Hemorrhagic stroke: introduction. Stroke 44:S65–S66. https://doi.org/10.1161/STROKEAHA.113.000856
3. Hermann DM, ElAli A (2012) The abluminal endothelial membrane in neurovascular remodeling in health and disease. Sci Signal 5:re4. https://doi.org/10.1126/scisignal.2002886
4. ElAli A, Hermann DM (2010) Apolipoprotein E controls ATP-binding cassette transporters in the ischemic brain. Sci Signal 3: ra72. https://doi.org/10.1126/scisignal.2001213
5. Sandoval KE, Witt KA (2008) Blood-brain barrier tight junction permeability and ischemic stroke. Neurobiol Dis 32:200–219. https://doi.org/10.1016/j.nbd.2008.08.005

6. Brouns R, Wauters A, De Surgeloose D, Marien P, De Deyn PP (2011) Biochemical markers for blood-brain barrier dysfunction in acute ischemic stroke correlate with evolution and outcome. Eur Neurol 65:23–31. https://doi.org/10.1159/000321965
7. Garbuzova-Davis S, Haller E, Williams SN, Haim ED, Tajiri N, Hernandez-Ontiveros DG, Frisina-Deyo A, Boffeli SM et al (2014) Compromised blood-brain barrier competence in remote brain areas in ischemic stroke rats at the chronic stage. J Comp Neurol 522:3120–3137. https://doi.org/10.1002/cne.23582
8. Lo EH (2008) A new penumbra: transitioning from injury into repair after stroke. Nat Med 14:497–500. https://doi.org/10.1038/nm1735
9. Wang X, Tsuji K, Lee SR, Ning M, Furie KL, Buchan AM, Lo EH (2004) Mechanisms of hemorrhagic transformation after tissue plasminogen activator reperfusion therapy for ischemic stroke. Stroke 35:2726–2730. https://doi.org/10.1161/01.STR.0000143219.16695.af
10. Del Zoppo GJ, Saver JL, Jauch EC, Adams HP Jr, American Heart Association Stroke C (2009) Expansion of the time window for treatment of acute ischemic stroke with intravenous tissue plasminogen activator: a science advisory from the American Heart Association/American Stroke Association. Stroke 40:2945–2948. https://doi.org/10.1161/STROKEAHA.109.192535
11. Sussman ES, Connolly ES Jr (2013) Hemorrhagic transformation: a review of the rate of hemorrhage in the major clinical trials of acute ischemic stroke. Front Neurol 4:69. doi: https://doi.org/10.3389/fneur.2013.00069
12. Zhang J, Yang Y, Sun H, Xing Y (2014) Hemorrhagic transformation after cerebral infarction: current concepts and challenges. Ann Transl Med 2(81). https://doi.org/10.3978/j.issn.2305-5839.2014.08.08
13. Clevers H, Nusse,R (2012) Wnt/beta-catenin signaling and disease. Cell 149:1192–1205. doi: https://doi.org/10.1016/j.cell.2012.05.012
14. Liebner S, Corada M, Bangsow T, Babbage J, Taddei A, Czupalla CJ, Reis M, Felici A et al (2008) Wnt/beta-catenin signaling controls development of the blood-brain. J Cell Biol 183:409–417. https://doi.org/10.1083/jcb.200806024
15. Tran KA, Zhang X, Predescu D, Huang X, Machado RF, Gothert JR, Malik AB, Valyi-Nagy T et al (2016) Endothelial beta-catenin signaling is required for maintaining adult blood-brain barrier integrity and central nervous system homeostasis. Circulation 133:177–186. https://doi.org/10.1161/CIRCULATIONAHA.115.015982
16. Lengfeld JE, Lutz SE, Smith JR, Diaconu C, Scott C, Kofman SB, Choi C, Walsh CM et al (2017) Endothelial Wnt/beta-catenin signaling reduces immune cell infiltration in multiple sclerosis. Proc Natl Acad Sci U S A 114:E1168–E1177. https://doi.org/10.1073/pnas.1609905114
17. ElAli A, Urrutia A, Rubio-Araiz A, Hernandez-Jimenez M, Colado MI, Doeppner TR, Hermann DM (2012) Apolipoprotein-E controls adenosine triphosphate-binding cassette transporters ABCB1 and ABCC1 on cerebral microvessels after methamphetamine intoxication. Stroke 43:1647–1653. https://doi.org/10.1161/STROKEAHA.111.648923
18. Wang YZ, Yamagami T, Gan Q, Wang Y, Zhao T, Hamad S, Lott P, Schnittke N et al (2011) Canonical Wnt signaling promotes the proliferation and neurogenesis of peripheral olfactory stem cells during postnatal development and adult regeneration. J Cell Sci 124:1553–1563. https://doi.org/10.1242/jcs.080580
19. Zhao Y, Wei ZZ, Zhang JY, Zhang Y, Won S, Sun J, Yu SP, Li J et al (2017) GSK-3β inhibition induced neuroprotection, regeneration, and functional recovery after intracerebral hemorrhagic stroke. Cell Transplant 26:395–407. https://doi.org/10.3727/096368916X694364
20. Jean LeBlanc N, Guruswamy R, ElAli A (2018) Vascular endothelial growth factor isoform-B stimulates neurovascular repair after ischemic stroke by promoting the function of pericytes via vascular endothelial growth factor receptor-1. Mol Neurobiol 55:3611–3626. https://doi.org/10.1007/s12035-017-0478-6
21. Ben-Zvi A, Lacoste B, Kur E, Andreone BJ, Mayshar Y, Yan H, Gu C (2014) Mfsd2a is critical for the formation and function of the blood-brain barrier. Nature 509:507–511. https://doi.org/10.1038/nature13324
22. Reese TS, Karnovsky MJ (1967) Fine structural localization of a blood-brain barrier to exogenous peroxidase. J Cell Biol 34:207–217
23. ElAli A, Doeppner TR, Zechariah A, Hermann DM (2011) Increased blood-brain barrier permeability and brain edema after focal cerebral ischemia induced by hyperlipidemia: role of lipid peroxidation and calpain-1/2, matrix metalloproteinase-2/9, and RhoA overactivation. Stroke 42:3238–3244. https://doi.org/10.1161/STROKEAHA.111.615559
24. Bordeleau M, ElAli A, Rivest S (2016) Severe chronic cerebral hypoperfusion induces microglial dysfunction leading to memory loss in APPswe/PS1 mice. Oncotarget 7:11864–11880. https://doi.org/10.18632/oncotarget.7689
25. ElAli A, Bordeleau M, Thériault P, Filali M, Lampron A, Rivest S (2016) Tissue-plasminogen activator attenuates Alzheimer's disease-related pathology development in APPswe/PS1 mice. Neuropsychopharmacology. 41:1297–1307. https://doi.org/10.1038/npp.2015.279
26. Brown RC, Morris AP, O'Neil RG (2007) Tight junction protein expression and barrier properties of immortalized mouse brain microvessel endothelial cells. Brain Res 1130:17–30. https://doi.org/10.1016/j.brainres.2006.10.083
27. Taddei A, Giampietro C, Conti A, Orsenigo F, Breviario F, Pirazzoli V, Potente M, Daly C et al (2008) Endothelial adherens junctions control tight junctions by VE-cadherin-mediated upregulation of claudin-5. Nat Cell Biol 10:923–934. https://doi.org/10.1038/ncb1752
28. Li VS, Ng SS, Boersema PJ, Low TY, Karthaus WR, Gerlach JP, Mohammed S, Heck AJ et al (2012) Wnt signaling through inhibition of beta-catenin degradation in an intact Axin1 complex. Cell 149:1245–1256. https://doi.org/10.1016/j.cell.2012.05.002
29. Benchenane K, Berezowski V, Fernández-Monreal M, Brillault J, Valable S, Dehouck MP, Cecchelli R, Vivien D et al (2005) Oxygen glucose deprivation switches the transport of tPA across the blood-brain barrier from an LRP-dependent to an increased LRP-independent process. Stroke 36:1065–1070
30. Abu Fanne R, Nassar T, Yarovoi S, Rayan A, Lamensdorf I, Karakoveski M, Vadim P, Jammal M et al (2010) Blood-brain barrier permeability and tPA-mediated neurotoxicity. Neuropharmacology. 58:972–980. https://doi.org/10.1016/j.neuropharm.2009.12.017.
31. Hawkins BT, Davis TP (2005) The blood-brain barrier/neurovascular unit in health and disease. Pharmacol Rev 57:173–185. https://doi.org/10.1124/pr.57.2.4
32. Cramer SC, Chopp M (2000) Recovery recapitulates ontogeny. Trends Neurosci 23:265–271
33. Knecht T, Story J, Liu J, Davis W, Borlongan CV, Dela Pena IC (2017) Adjunctive therapy approaches for ischemic stroke: innovations to expand time window of treatment. Int J Mol Sci 18:E2756. https://doi.org/10.3390/ijms18122756
34. Larrue V, von Kumme R, Del Zoppo G, Bluhmki E (1997) Hemorrhagic transformation in acute ischemic stroke. Potential contributing factors in the European Cooperative Acute Stroke Study. Stroke 28:957–960
35. Zhao BQ, Wang S, Kim HY, Storrie H, Rosen BR, Mooney DJ, Wang X, Lo EH (2006) Role of matrix metalloproteinases in

delayed cortical responses after stroke. Nat Med 12:441–445. https://doi.org/10.1038/nm1387

36. Wang W, Li M, Wang Y, Wang Z, Zhang W, Guan F, Chen Q, Wang J (2017) GSK-3beta as a target for protection against transient cerebral ischemia. Int J Med Sci 14:333–339. https://doi.org/10.7150/ijms
37. Carson-Walter EB, Hampton J, Shue E, Geynisman DM, Pillai PK, Sathanoori R, Madden SL, Hamilton R et al (2005) Plasmalemmal vesicle associated protein-1 is a novel marker implicated in brain tumor angiogenesis. Clin Cancer Res 11:7643–7650. https://doi.org/10.1158/1078-0432.CCR-05-1099
38. Shue EH, Carson-Walter EB, Liu Y, Winans BN, Ali ZS, Chen J, Walter KA (2008) Plasmalemmal vesicle associated protein-1 (PV-1) is a marker of blood-brain barrier disruption in rodent models. BMC Neurosci 9:29. https://doi.org/10.1186/1471-2202-9-29
39. Wang YF, Tsirka SE, Strickland S, Stieg PE, Soriano SG, Lipton SA (1998) Tissue plasminogen activator (tPA) increases neuronal damage after focal cerebral ischemia in wild-type and tPA-deficient mice. Nat Med 4:228–231
40. Wang W, Li M, Wang Y, Li Q, Deng G, Wan J, Yang Q, Chen Q et al (2016) GSK-3beta inhibitor TWS119 attenuates rtPA-induced hemorrhagic transformation and activates the Wnt/beta-catenin signaling pathway after acute ischemic stroke in rats. Mol Neurobiol 53:7028–7036. https://doi.org/10.1007/s12035-015-9607-2
41. Soeteman DI, Menzies NA, Pandya A (2017) Would a large tPA trial for those 4.5 to 6.0 hours from stroke onset be good value for information? Value Health 20:894–901. https://doi.org/10.1016/j.jval.2017.03.004